BRAIN RESEARCH 1347 (2010) 111–124

available at www.sciencedirect.com

ScienceDirect

www.elsevier.com/locate/brainres

BRAIN RESEARCH

Research Report

Analysis of the cholinergic pathology in the P301L tau transgenic pR5 model of tauopathy

C. Köhler[a,*], P. Bista[a], J. Götz[b], H. Schröder[a]

[a]Dept. of Anatomy/Neuroanatomy, University Hospital Cologne, Cologne, Germany
[b]Alzheimer's and Parkinson's Disease Laboratory, Brain and Mind Research Institute, University of Sydney, Sydney, NSW, Australia

ARTICLE INFO

Article history:
Accepted 24 May 2010
Available online 1 June 2010

Keywords:
Alzheimer's disease
Tau
Cholinergic

ABSTRACT

Cholinergic deafferentation of telencephalon is a major factor contributing to cognitive impairment in Alzheimer's disease. There is evidence that the degeneration of cholinergic fibers which innervate the cortex and hippocampus is due to the development of neurofibrillary tangles in the perikarya of origin. Neurofibrillary tangle formation has been modeled in the transgenic pR5 mouse strain that overexpresses the longest human tau isoform together with the P301L mutation that has been previously identified in familial cases of frontotemporal dementia and parkinsonism linked to chromosome 17 (FTDP-17). To test the suitability of the pR5 model as a model of Alzheimer's disease concerning the cholinergic innervation of the telencephalon, we determined the expression of the human tau transgene and the presence of neurofibrillary changes in the basal nucleus of Meynert, the septal nuclei and the diagonal band of Broca, sources of cholinergic innervation of the cerebral cortex and hippocampus. We found that the cholinergic neurons of these nuclei, despite widespread expression of the human tau transgene, neither expressed human tau nor displayed immunoreactivity with antibodies AT8 and AT180 which recognize hyperphosphorylated tau. Immunoreactivity for choline-acetyl transferase did not reveal significant differences between pR5 mice and non-transgenic littermates in the basal forebrain, cortex and hippocampus. However, in the amygdala dystrophic cholinergic neurites were observed which were not present in non-transgenic mice. Our data show that although pR5 mice develop neurofibrillary lesions, they do not model the degeneration of basal forebrain cholinergic neurons observed in Alzheimer's disease.

1. Introduction

Two different pathogenetic mechanisms are closely related to cognitive impairment in AD. Firstly, entorhinal layer II neurons degenerate in AD with the development of NFTs as a major neuropathological alteration (Braak and Braak, 1991; Gómez-Isla et al., 1996). NFTs are composed of fibrillar forms of the microtubule-associated protein tau. The axons of the entorhinal layer II neurons give rise to the perforant path which projects to the hippocampal dentate gyrus and the CA3 region (Witter, 1993),

* *Corresponding author*. Department of Anatomy, University Hospital of Cologne, Kerpener Straße 62, 50924 Cologne, Germany.
E-mail address: c.koehler@uni-koeln.de (C. Köhler).

Abbreviations: AD, Alzheimer's disease; APP, amyloid precursor protein; ChAT, choline-acetyl transferase; FDTP-17, frontotemporal dementia and parkinsonism linked to chromosome 17; HDB, horizontal limb of the diagonal band of Broca; ir, immunoreactive; LS, lateral septal nucleus; MS, medial septum; NbM, basal nucleus of Meynert/nucleus basalis magnocellularis; NFTs, Neurofibrillary tangles; non-tg, non-transgenic; VDB, vertical limb of the diagonal band

0006-8993/$ – see front matter © 2010 Elsevier B.V. All rights reserved.
doi:10.1016/j.brainres.2010.05.076

thus, in AD, an important segment of the structural basis of short-term memory becomes disrupted (Hyman et al., 1984, 1990; Braak and Braak, 1993). Secondly, there is shrinkage (Pearson et al., 1983) and loss of cholinergic perikarya in the NbM (Whitehouse et al., 1982) as well as loss of their terminal projections to the cerebral cortex which leads to an impairment of acetylcholine-mediated modulation in cortical neurotransmission (McGehee et al., 1995; Efange et al., 1997). Reduced cortical ChAT-activity (Perry et al., 1981; DeKosky et al., 1992; Bierer et al., 1995) and neuropathological changes in the NbM (Iraizoz et al., 1999) have been shown to correlate with the severity of dementia. For the neurons in the NbM, too, evidence has been presented that their degeneration is associated with neurofibrillary changes (Saper et al., 1985; Cullen and Halliday, 1998; Mesulam et al., 2004). Cytoskeletal changes in the NbM are morphologically different from cortical NFTs in displaying a spherical appearance. They are already present in stage I of cortical neurofibrillary pathology and develop in parallel with cortical neurodegeneration (Sassin et al., 2000, but see Cullen and Halliday, 1998).

One way to model the cholinergic deficit in AD is to experimentally lesion the cholinergic innervation of rats by stereotactic targeting or injection of IgG-saporin. This causes learning impairments, which were attributed to deficits in regulating attention rather than in memory itself (Chiba et al., 1999; Galani et al., 2002). Direct lesioning of the cholinergic afferents in the posterior parietal cortex, for example, results in a failure to increase attention to a conditioned stimulus (Bucci et al., 1999), whereas a selective lesion of ChAT-positive neurons in the MS and VDB which innervate the hippocampus disrupts decrements of conditioned stimulus processing (Baxter et al., 1997). In AD, the dual impairment of memory and regulation of attention (entorhinal and cholinergic lesions) may foster and aggravate cognitive decline (Sarter et al., 2003; Cassel et al., 2008). Lesioned rats, however, develop neither amyloid deposits nor neurofibrillary changes, both histopathological hallmarks of AD (reviewed in Gonzalez de Aguilar et al., 2008; Cassel et al., 2008).

Reversible hyperphosphorylation of tau in basal forebrain cholinergic neurons in Syrian hamsters during hibernation has been reported (Härtig et al., 2007; Su et al., 2008), but this physiological regulatory mechanism does not seem to proceed to the formation of tangles and does not allow behavioral testing of the animals when tau is hyperphosphorylated.

As a transgenic animal model may come closer to the changes in the human NbM, we analyzed the pR5 mouse strain, a well established model of tauopathy which develops NFTs due to overexpression of the longest human tau (htau) isoform (2^+3^+4R) together with the P301L mutation, under control of the neuron-specific mThy1.2 promoter (Götz et al., 2001; Pennanen et al., 2004). The P301L mutation causes early-onset FDTP-17 in humans (Hutton et al., 1998). pR5 mice have been established as a valuable model for AD, in combining the amyloid plaque and NFT pathology by generating triple transgenic mice resulting from a cross of pR5 mice with mutant APP and presenilin 2-expressing mice (Rhein et al., 2009; Grueninger et al., 2010). Here, we determined whether pR5 mice model the basal forebrain cholinergic lesion observed in AD by analyzing telencephalic cholinergic neurons in the NbM, septum, diagonal band and caudate–putamen for transgene expression and signs of neurodegeneration.

2. Results

2.1. *Cholinergic neurons of P301L tau transgenic pR5 mice appear normal*

The rodent equivalents of the primate NbM are the magnocellular nuclei in the ventral globus pallidus, the substantia innominata and the lateral preoptic area, collectively named nucleus basalis magnocellularis. We use in this report the abbreviation NbM also for the nucleus basalis magnocellularis. The NbM provides the major cholinergic innervation of the cerebral cortex and amygdala together with the HDB, whereas the vast majority of the cholinergic innervation of the hippocampus originates in the MS and VDB. The distribution of cholinergic neurons in the basal forebrain of pR5 mice revealed by ChAT-immunoreactivity was in line with previous studies in rodents (Nagai et al., 1982; McKinney et al., 1983; Satoh et al., 1983; Carlsen et al., 1985; Kitt et al., 1994).

At visual examination, ChAT-ir cholinergic neurons in the NbM exhibited no obvious differences in distribution, morphology or staining intensity between pR5 mice and non-tg littermates. This was confirmed by cell counts in sections at three levels relative to Bregma which revealed no significant differences between both groups of mice (number/level, means ± SEM: non-tg = 77 ± 7.07, 50.67 ± 2.84, 37.50 ± 2.67, pR5 = 77.17 ± 5.43, 47.67 ± 3.10, 42.5 ± 3.15) (Fig. 1). The analysis of the area of individual ChAT-ir profiles in the NbM also revealed no significant differences (area, mean ± SEM: non-tg = 79.70 ± 2.10 μm^2; pR5 = 84.42 ± 2.23 μm^2). The representation of the data in box plots (not shown) or histograms (Fig. 2) showed a similar distribution. The distributions were compared using the Kolmogrov–Smirnov test which resulted in a P value of 0.131 indicating a similar spectrum of profile sizes in both groups of mice.

Within the MS, cholinergic neurons were distributed in pR5 mice and non-tg littermates in an inverted V shaped pattern. The VDB continues caudally from the MS in a vertical fashion before separating into two HDBs. ChAT-immunoreactivity of the neuronal perikarya in the MS and VDB appeared similar in pR5 mice and non-tg littermates. Numbers of cholinergic neurons in the MS and VBD at all three levels relative to Bregma examined were not significantly different between pR5 mice and non-tg littermates (number/level, means ± SEM: non-tg = 46.8 ± 3.01, 61.2 ± 4.75, 45.6 ± 3.70, pR5 = 49.4 ± 5.81, 62.2 ± 3.53, 43.6 ± 2.54) (Fig. 3). The same was found for the mean area of ChAT-ir profiles (area, mean ± SEM: non-tg = 77.63 ± 1.84 μm^2; pR5 = 76.85 ± 1.80 μm^2). Again, the data appeared similarly distributed (Fig. 4) which was confirmed by the Kolmogrov–Smirnov test ($P = 0.553$).

The LS can be subdivided into dorsal, intermediate and ventral nuclei (Swanson and Cowan, 1979). Perikarya of cholinergic neurons were present in the LS at Bregma positions 0.74 to 0.14. These neurons lay mainly in the intermediate part of the LS, but ventrally they were relatively scarce and dorsally, the lowest numbers were observed. Their staining intensity was faint as compared to those present in the MS. Numbers, morphology and staining intensity of these cholinergic neurons were comparable between pR5 mice and non-tg littermates (Fig. 3). The staining intensity of ChAT-ir neurons in the HDB was intense in both the pR5 mice and non-tg littermates (not shown).

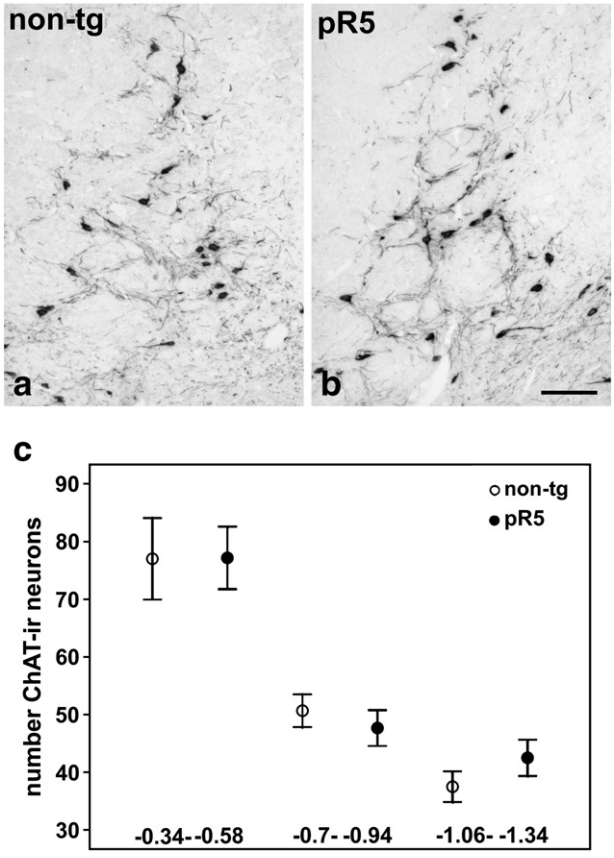

Fig. 1 – Distribution and numbers of cholinergic neurons in the lateral globus pallidus and substantia innominata of P301L tau transgenic pR5 mice. (a, b) 4% PFA-fixed, 5 μm thick, coronal sections obtained from an age- and gender-matched pR5 mouse and non-tg littermate. ChAT-ir, cholinergic neurons located in the left lateral globus pallidus and substantia innominata appear similar in distribution, morphology and staining intensity. (c) There is no significant difference in the number of ChAT-ir neuronal perikarya at each of the three levels relative to the Bregma analyzed. The positions of the sections relative to the Bregma are indicated below the respective values. Values represent means ± SEM of six mice per group. Scale bar a, b 100 μm.

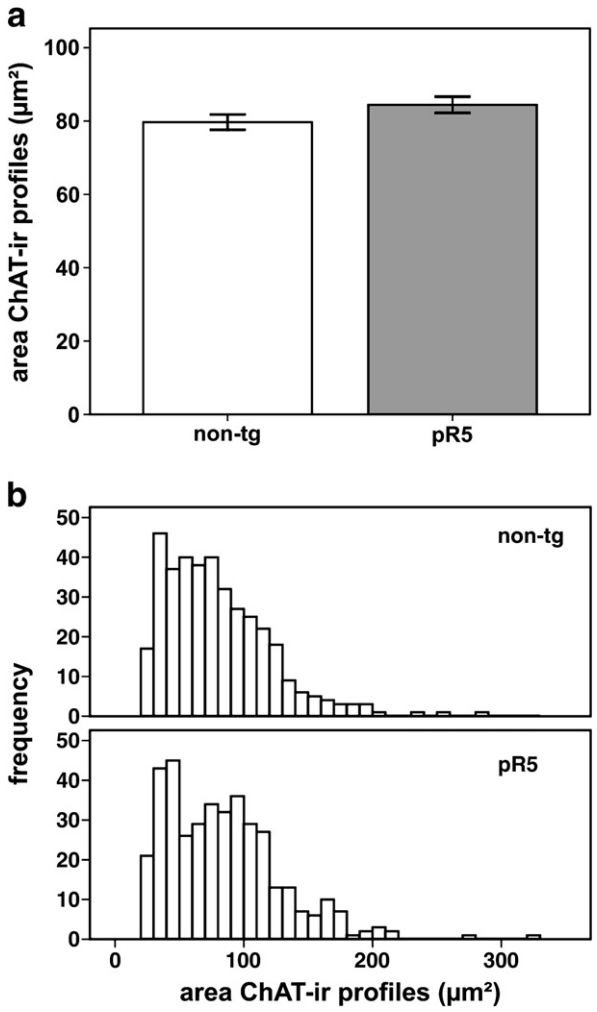

Fig. 2 – Quantification of ChAT-immunoreactivity in the lateral globus pallidus and substantia innominata from both sides. (a) There is no significant difference between the mean area of individual ChAT-ir profiles of non-tg and pR5 mice analyzed at position –0.7 to –0.94 relative to Bregma. Values represent means ± SEM of 379 and 388 profiles respectively. Profiles smaller than 100 pixel (=26.99 μm²) which morphologically appear as small fragments of cells were excluded from the analysis. (b) The histogram shows a similar distribution of ChAT-ir profiles in the lateral globus pallidus and substantia innominata in non-tg and pR5 mice.

Terminal processes of basal forebrain cholinergic neurons in the cerebral cortex and hippocampus of pR5 mice and non-tg littermates appeared similar (Fig. 5). Contrary to Satoh et al. (1983) and Kitt et al. (1994) we frequently observed small ChAT-ir neurons in upper cortical layers often displaying a clear bipolar morphology in both groups of mice. Moderately enlarged, spherical ChAT-ir structures reminiscent of dystrophic cholinergic neurites were rare in the cortex and hippocampus of both pR5 mice and non-tg littermates. The lateral and basolateral amygdaloid nuclei of pR5 mice contained cluster of vacuolated, enlarged, ChAT-ir terminals, which were not observed in non-tg littermates. They were not frequent but occasionally seen in four out of six mice; in two mice in the lateral and in two mice in the basolateral amygdaloid nuclei (Fig. 6).

2.2. *Lack of expression of htau in cholinergic neurons of pR5 mice*

The HT7 antibody specifically recognizes htau independent of the state of phosphorylation and thus can be used to visualize those neurons in the pR5 brain that express the human tau transgene (Götz et al., 2001). The extent of HT7-immunoreactivity varied between individual mice, but all mice examined showed the same pattern of expression. Within the cell clusters of the NbM, HT7-ir was generally absent (Fig. 7); only very few HT7-ir neuronal perikarya were found and only in those mice that displayed a generally strong HT7-immunoreactivity. HT7-ir neuronal perikarya were not seen in the MS

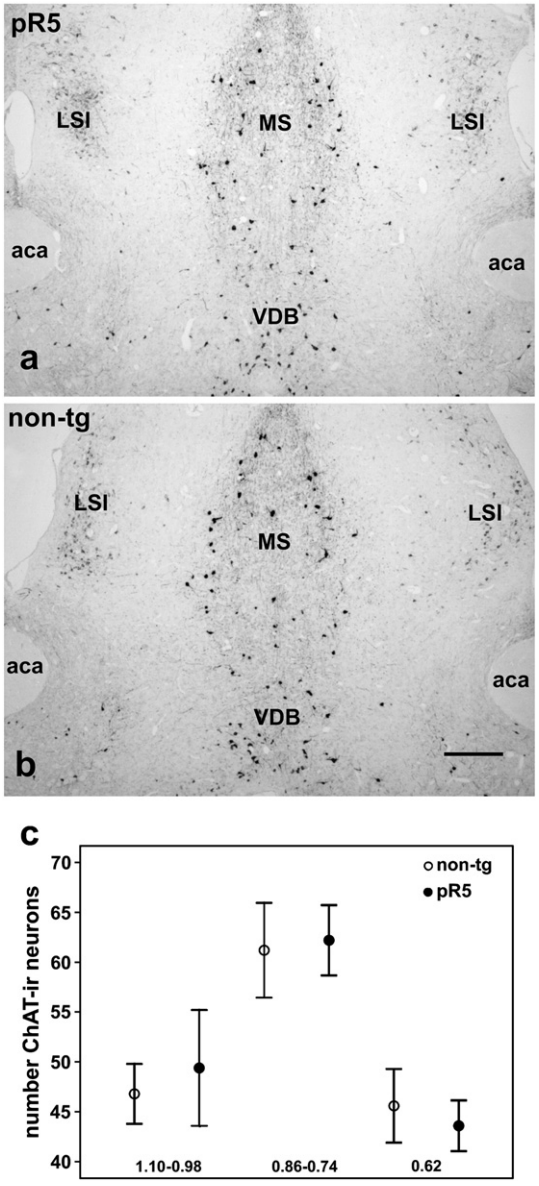

Fig. 3 – Distribution and numbers of cholinergic neurons in the septum of P301L tau transgenic pR5 mice. a, b 4% PFA-fixed, 5 μm thick, coronal sections from a pR5 mouse (a) and age- and gender-matched non-tg littermate (b). ChAT-ir, cholinergic neurons in the medial septum (MS), intermediate part of the lateral septum (LSI) and vertical limb of the diagonal band (VDB) appear similar in distribution, morphology and staining intensity. ChAT-ir, cholinergic neurons in the LSI of both groups are less intensively stained. (c) There is no significant difference in the number of ChAT-ir neuronal perikarya at each of the three levels relative to Bregma analyzed. The positions of the sections relative to the Bregma are indicated below the respective values. Values represent means ± SEM of five mice per group. aca anterior commissure, anterior. Scale bar a, b 200 μm.

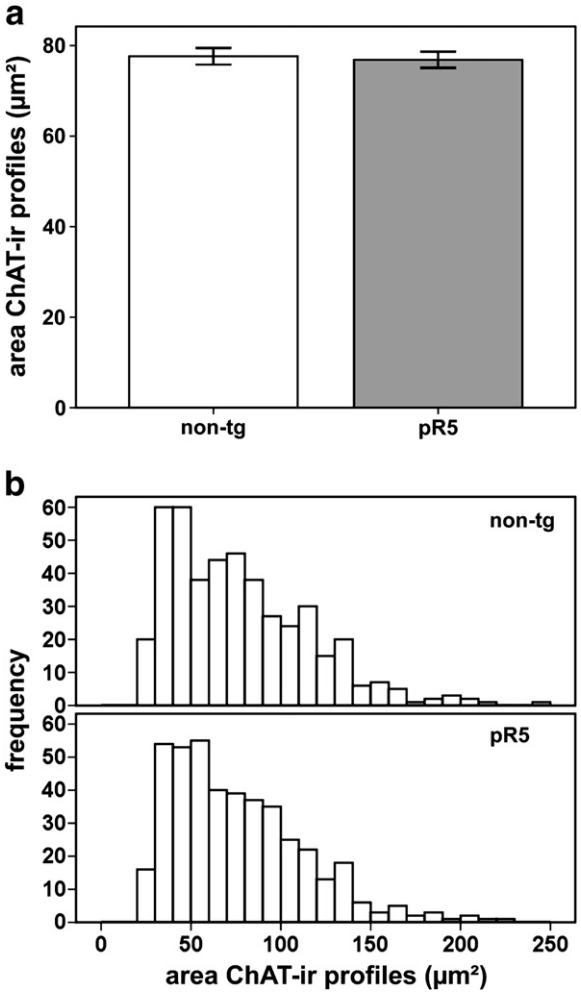

Fig. 4 – Quantification of ChAT-immunoreactivity in the medial septum and vertical limb of the diagonal band. (a) There is no significant difference between the mean area of individual ChAT-ir profiles of non-tg and pR5 mice analyzed at position 0.86 to 0.74 relative to Bregma. Values represent means ± SEM of 450 and 431 profiles respectively. Profiles smaller than 100 pixel (=26.99 μm²) were excluded from the analysis. (b) The histogram shows a similar distribution of ChAT-ir profiles in the medial septum and vertical limb of the diagonal band in non-tg and pR5 mice.

(Fig. 8). In the dorsal LS, a few HT7-ir neuronal perikarya were present, increasing in numbers posteriorly. Both the VDB and HDB did not stain with the HT7 antibody (not shown).

2.3. *Hyperphosphorylation of tau is not detectable in cholinergic neurons of pR5 mice*

pR5 mice are characterized by hyperphosphorylation of tau at many epitopes including AT8 (S202/T205) and AT180 (T231/S235) in many regions of the brain (Götz et al., 2001; Deters et al., 2008). However, within the cell clusters of the NbM, there were no neuronal perikarya displaying tau hyperphosphorylation at either epitope, except for sporadic neurons (Fig. 7). To investigate whether these AT8- and AT180-positive neurons are cholinergic, double staining for AT8 or AT180 and ChAT was performed, however, no co-localization was found (Fig. 9a).

In the MS, three of six pR5 mice displayed AT180-immunolabeling of neuronal perikarya, while AT8-immunolabeled

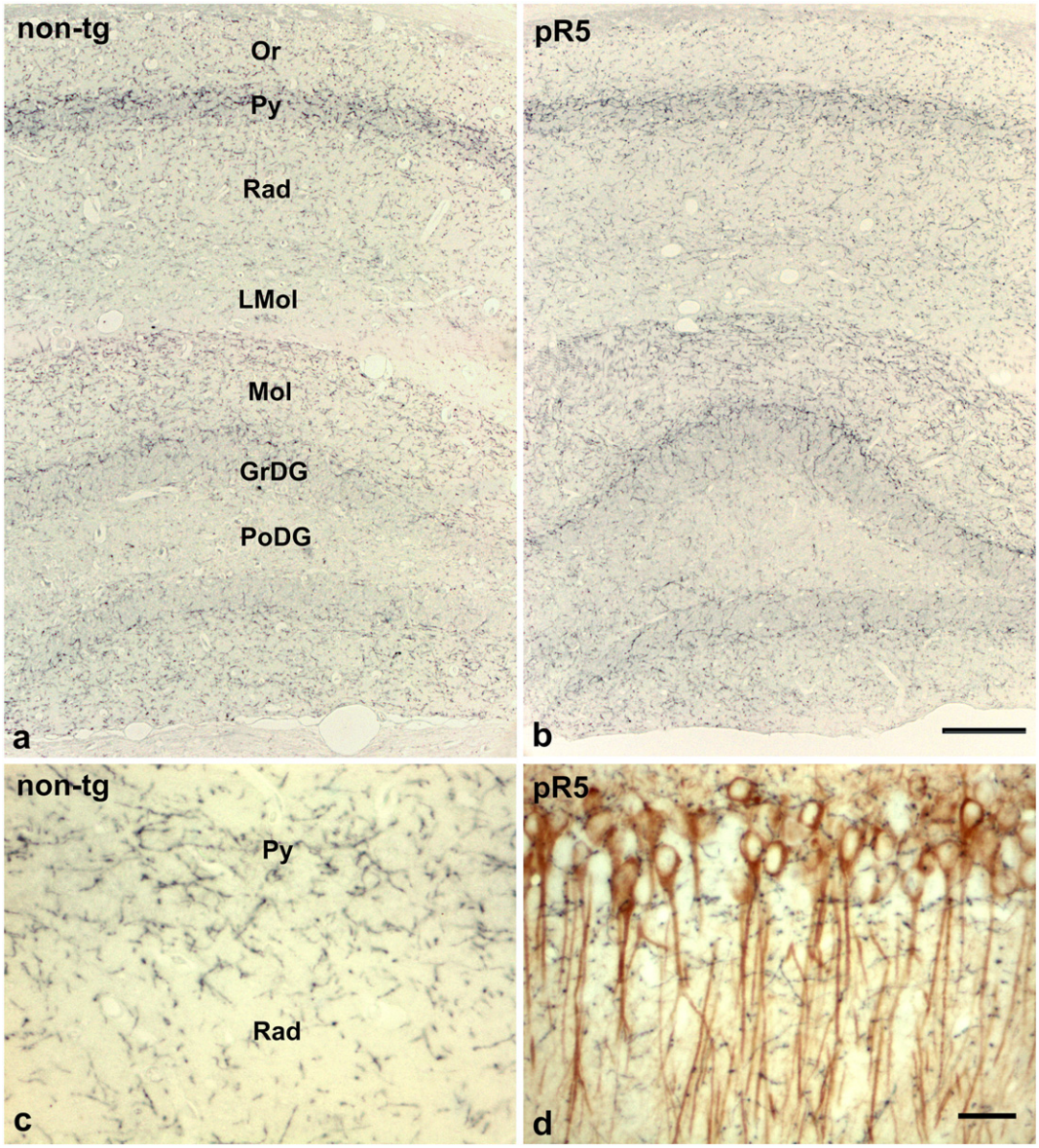

Fig. 5 – Terminal cholinergic fibers in the hippocampus of P301L tau transgenic pR5 mice. 4% PFA-fixed, 5 μm thick, coronal sections from a non-tg littermate (a, c) and age- and gender-matched pR5 mouse (b, d). (a, b) ChAT-ir, cholinergic fibers in the hippocampus of non-tg littermates and pR5 mice appear similar in distribution and density. (c) A section from a non-tg littermate consecutively stained for ChAT and with antibody AT180 shows cholinergic fibers around CA1 pyramidal cells at higher magnification and the absence of AT180-immunoreactivity. (d) An area corresponding to c from a pR5 hippocampus showing a similar plexus of cholinergic fibers and widespread AT180-immunoreactivity in perikarya and dendrites of CA1 pyramidal cells. GrDG granular layer of dentate gyrus, LMol lacunosum moleculare layer, Mol molecular layer of dentate gyrus, or oriens layer, PoDG polymorph layer of dentate gyrus, py pyramidal cell layer, rad stratum radiatum. Scale bar a, b 100 μm and c, d 20 μm.

neuronal perikarya were observed only in one of the AT180-ir mice (Fig. 8). These neurons were not cholinergic as determined by double staining for AT8 or AT180 and ChAT (Figs. 9b, c). In the dorsal LS, a few AT8 and AT180-ir neuronal perikarya were present, increasing in numbers posteriorly similar to HT7-ir neuronal perikarya. As for the MS, there was more AT180- than AT8-immunoreactivity: five out of six mice examined showed AT180-ir perikarya while only three mice showed AT8-ir neuronal perikarya. Again, these neurons were not ChAT-ir (not shown). In addition to neuronal perikarya, the LS contained HT7-, AT8-, and AT180-ir fibers (Fig. 8). For comparison, in the rat, fibers in the LS were shown to originate from hippocampal pyramidal cells of all CA fields (Swanson and Cowan, 1979). CA pyramidal neurons of pR mice strongly express htau suggesting that the HT7-, AT8-, and AT180-ir fibers in the LS are projections from htau-expressing neurons located in the hippocampus (Deters et al., 2008; own unpublished observations).

For both the VDB and HDB of pR5 mice, AT8 and AT180 antibodies revealed few immunoreactive neurons (not shown). AT180-immunolabeled neurons were seen in the VDB and HDB of all pR5 mice examined, but AT8-immunolabeled neurons were observed in only one out of six mice.

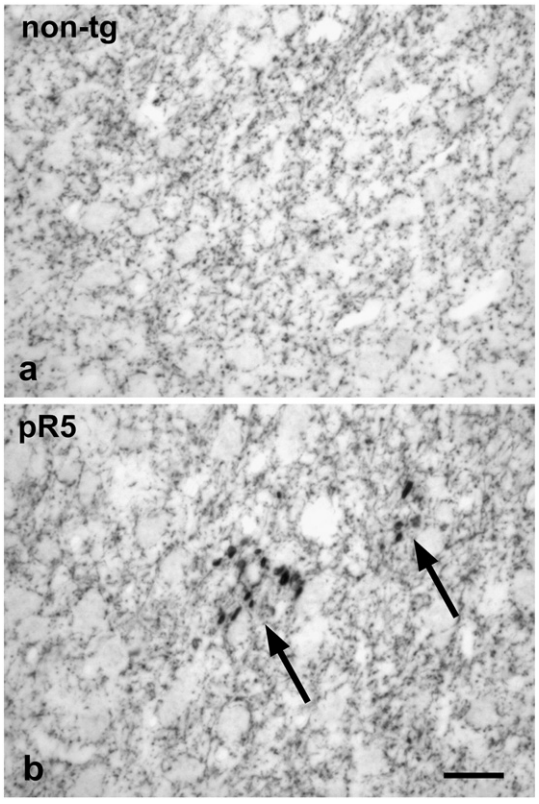

Fig. 6 – Terminal cholinergic fibers in the basolateral amygdaloid nucleus of P301L tau transgenic pR5 mice. 4% PFA-fixed, 5 μm thick, coronal sections from a non-tg littermate (a) and age- and gender-matched pR5 mouse (b). (a, b) ChAT-ir, cholinergic fibers in the basolateral amygdaloid nucleus of non-tg littermates and pR5 mice appear similar in distribution and density, but clusters of enlarged cholinergic fibers (arrows) are only present in pR5 mice. Scale bar 20 μm.

2.4. *Lack of expression in the caudate–putamen*

We also included cholinergic interneurons of the caudate–putamen in our investigation. These interneurons neither expressed htau nor displayed AT8- or AT180-immunoreactivity, while bundles of fibers were immunoreactive with HT7 and AT180 (Fig. 10). These fibers are likely to originate from the neocortex, mainly from lamina V neurons, as shown for the rat (McGeorge and Faull, 1989). Likewise, HT7- and AT180-ir fibers in the lateral globus pallidus and internal capsule (Fig. 7) may originate in the cortex (Naito and Kita, 1994; Zaborszky et al., 1997). In line with this, cortical neurons of pR5 mice, located in layer V of isocortical areas, express htau (are HT7-ir) and display AT8- and AT180-immunoreactivity (Fig. 10). The immunohistochemical results are summarized in Table 1.

3. Discussion

Of the mutations leading to FTDP-17 in humans, the P301L mutation is the most frequent exonic mutation, leading to a neuronal and glial pathology (Mirra et al., 1999; Reed et al., 2001; Miyasaka et al., 2001; Wszołek et al., 2005; Whitwell et al., 2009). The pathology caused by the P301L mutation in humans varies. Severe affection of the frontal and temporal lobes is most consistently seen. Greater loss of gray matter has been observed in the lateral temporal lobes whereas the medial temporal lobes are relatively spared (Whitwell et al., 2009). The involvement of the entorhinal cortex, hippocampus and amygdala is variable (Reed et al., 2001). Typically there is a degeneration of the upper cortical layers (Reed et al., 2001; Miyasaka et al., 2001; Wszołek et al., 2005). Two reports mention the affection of the NbM or substantia innominata by this mutation (Nasreddine et al., 1999; Bird et al., 1999; reviewed in Wszołek et al., 2005).

Using HT7-immunoreactivity, in human P301L mutant tau expressing pR5 mice, we did not observe expression of human tau in cholinergic neurons of the NbM, MS, LS, diagonal band of Broca and caudate–putamen, but in keeping with previous studies there was strong expression of the transgene in the amygdala, hippocampus and cortical layers V and VI (Götz et al., 2001; Pennanen et al., 2004; Deters et al., 2008). This differential pattern of transgene expression is in part caused by the insertion site of the transgene (Wallace et al., 2000; Houdebine, 2002). It is also determined by the mThy1.2 promoter and other sequence elements on the expression vector that has been used to drive expression of the transgene in the pR5 mice. In K369I mutant tau expressing K3 mice, in comparison, that used the same expression vector, the transgene is in addition expressed in the substantia nigra pars compacta, resulting in parkinsonism as a defining feature; this is likely due to a unique integration site of the transgene (Ittner et al., 2008, 2009). Comparison of the expression pattern of htau in pR5 mice, however, with that of GAP-43 or CAP-23, also driven by the mThy1.2 promoter, in adult mice from a total of eight transgenic lines (Caroni, 1997) reveals several similarities. Across all lines, strong expression was observed in the amygdala and hippocampus. In the cerebral cortex expression was most consistently seen in cortical layers V and VI. There was little expression in the hypothalamus and in four of the eight strains examined the transgene was not expressed in the caudate–putamen. In the brainstem the transgene was consistently expressed e.g. in the motor nucleus of the trigeminus where we also observed a marked HT7-immunoreactivity in pR5 mice (own unpublished results).

Closely following the distribution of HT7-immunoreactivity, hyperphosphorylation of tau in the basal forebrain was nearly absent from the NbM, MS, intermediate and ventral parts of the LS, VDB, HDB and caudate–putamen. We observed AT8- and AT180-immunoreactivity of a few non-cholinergic cells in the NbM, MS and diagonal band without corresponding HT7-staining which may be due to hyperphosphorylation of endogenous mouse tau which shares phospho-epitopes with human tau (Kurt et al., 2001), or levels of htau may have been too low to be detected with HT7. As shown for the basal forebrain of the rat, subpopulations of neurons expressing different calcium binding proteins are distributed throughout cholinergic nuclei. Whereas parvalbumin-containing neurons are mainly large cells, the calbindin- and calretinin-expressing subpopulations include small to medium-sized neurons (Gritti et al., 2003). These appear morphologically similar to the cells which display hyperphosphorylated tau in this study.

In all pR5 mice examined, AT8-immunoreactivity was less pronounced in the basal forebrain when compared to AT180-

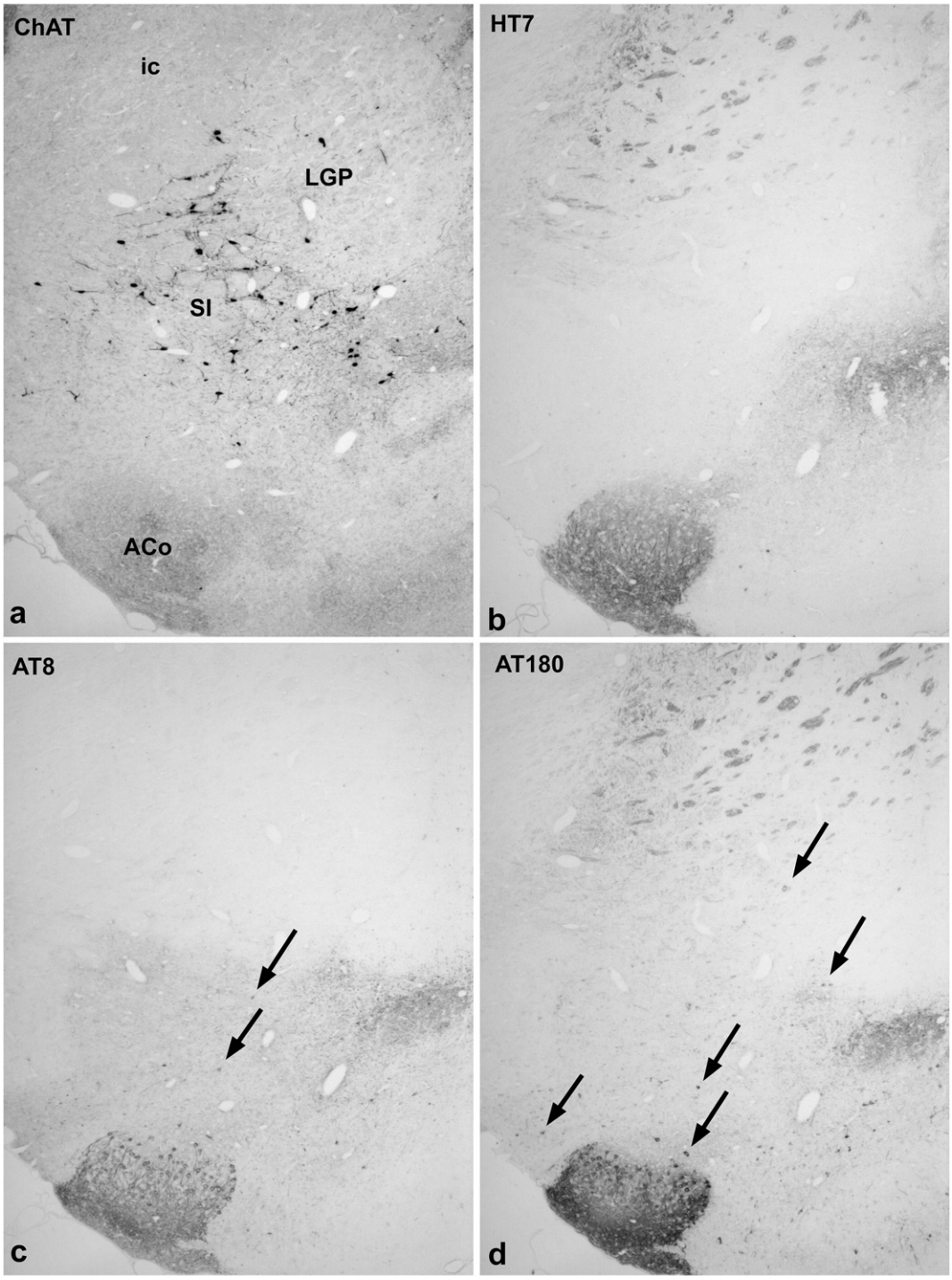

Fig. 7 – Expression of human tau and hyperphosphorylation of tau in the lateral globus pallidus and substantia innominata of P301L tau transgenic pR5 mice. a–d 4% PFA-fixed, 5 μm thick, coronal sections through the left basal forebrain of a pR5 brain showing: (a) ChAT-positive, cholinergic neurons located in the left lateral globus pallidus (LGP) and substantia innominata (SI); (b) lack of htau expression in cholinergic neurons, but expression in the anterior cortical amygdaloid nucleus (Aco) as well as its presence in fibers in the lateral globus pallidus and internal capsule (ic); (b, c, d) correspondence of htau expression to the presence of AT8- and AT180-epitopes and (c, d) the more widespread distribution of hyperphosphorylation at T231/S235 (AT180 epitope) compared to hyperphosphorylation at S202/T205 (AT8 epitope). Arrows point to examples of occasional neurons displaying hyperphosphorylated tau. Scale bar 200 μm.

immunoreactivity. This observation fits well with the time course and divergent pattern of the appearance of aberrant phospho-epitopes in the brains of pR5 mice for the amygdala, hippocampus and cortex as reported by Deters et al. (2008). The correspondence of HT7-, AT8-, and AT180-immunoreactivity suggests that with a few possible exceptions only those neurons

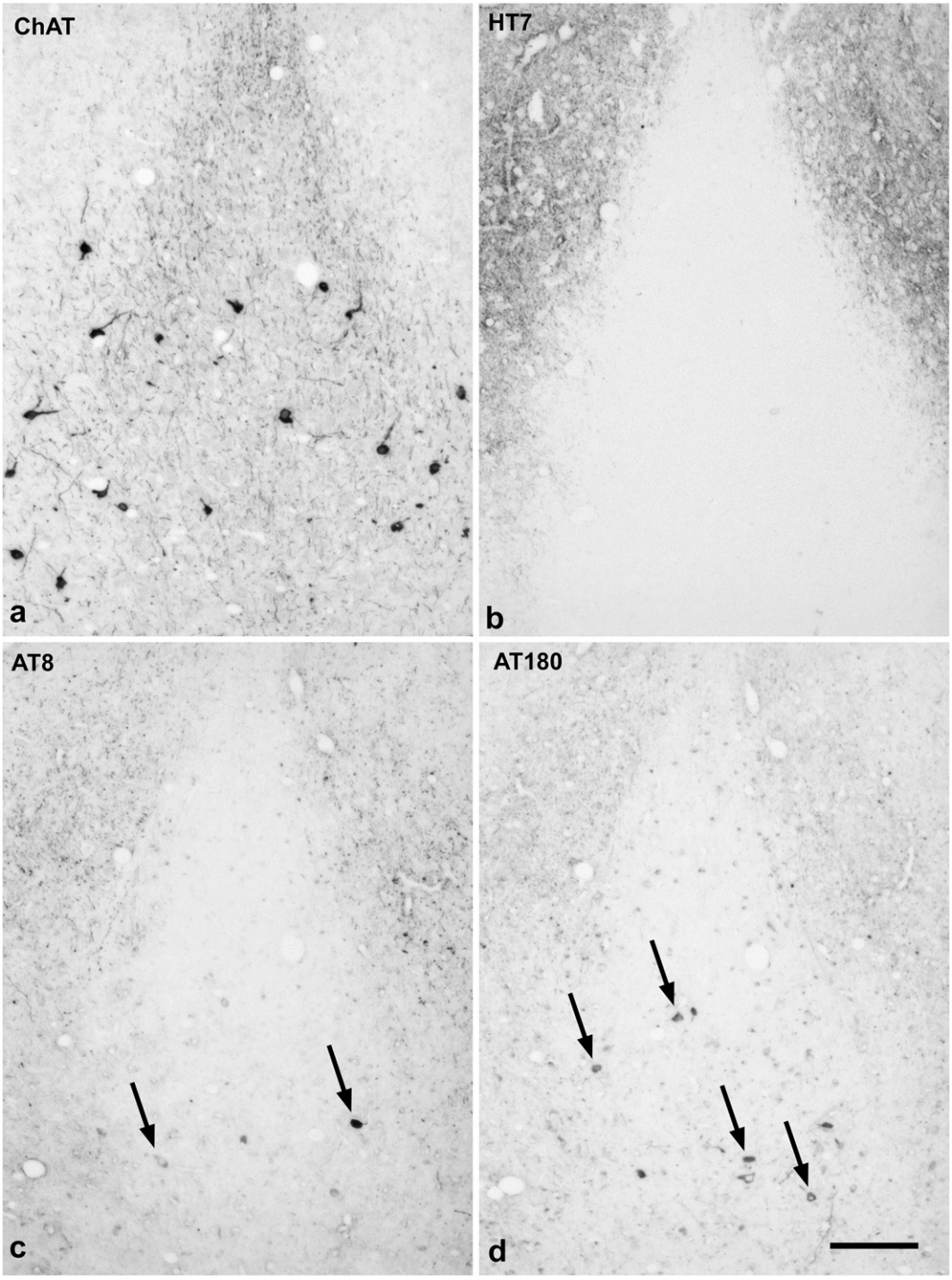

Fig. 8 – Human tau expression and hyperphosphorylation of tau in the septum of P301L tau transgenic pR5 mice. a–d 4% PFA-fixed, 5 μm thick, coronal sections through the septum of a pR5 brain. (a) ChAT-positive cholinergic neurons and processes are located in the medial septum. (b) htau is not expressed in the medial septum, but there is dense staining of processes in the lateral septum. (c) Occasional cells (arrows) display hyperphosphorylation at S202/T205 (AT8 epitope). There is also hyperphosphorylation at S202/T205 in processes in the lateral septum. (d) Compared to hyperphosphorylation at S202/T205, there are more cells showing hyperphosphorylation at T231/S235 (AT180 epitope) in the medial septum (arrows point to examples), but there is less staining of processes in the lateral septum. Scale bar a–d 100 μm.

in pR5 mice which express mutated htau at sufficiently high levels develop tau pathology. Taken together, our findings suggest that the distribution of hyperphosphorylated tau within the pR5 brain is mainly caused by properties of the promoter. A wide range of phenotypes in transgenic mice expressing htau with the P301L mutation demonstrates the impact of the

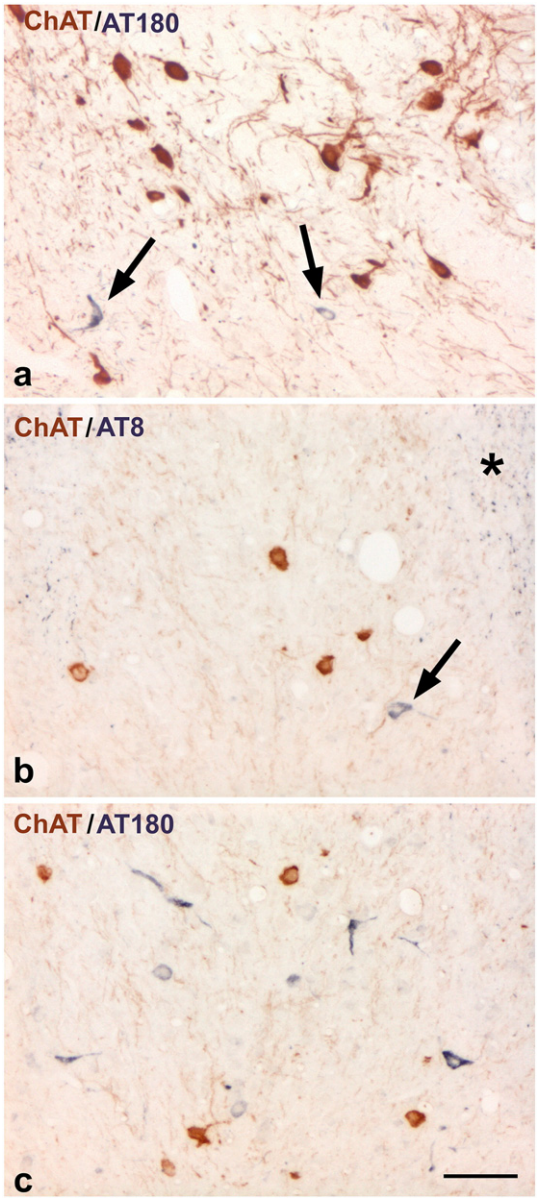

Fig. 9 – Neurons displaying hyperphosphorylation of tau in the substantia innominata and septum of P301L tau transgenic pR5 mice are not cholinergic. a–c 4% PFA-fixed, 5 μm thick, coronal sections through the right substantia innominata and medial septum of pR5 mice. (a) In the substantia innominata, occasional non-cholinergic neurons (arrows) display the AT180 epitope. (b) Occasional non-cholinergic neurons (arrows) in the medial septum display the AT8 epitope. There is also pronounced staining of fibers in the lateral septum (asterisks). (c) As shown by comparison to a consecutive section, numbers of AT180-ir neurons exceed those of AT8-ir neurons in the medial septum. Scale bar a–c 50 μm.

promoter used to drive transgene expression (Lewis et al., 2000; Ramsden et al., 2005; Murakami et al., 2006; reviewed in Götz and Ittner, 2008; Götz and Götz, 2009). Interestingly, the expression pattern of the transgene has been correlated with functional impairment: regions severely affected by neurofibrillary pathology in pR5 mice—such as the basolateral amygdaloid nucleus and hippocampus—have a crucial role in functions that are impaired in 6–11 month-old pR5 mice, as shown by an accelerated extinction of conditioned taste aversion and an impairment of spatial reference memory, while spatial working memory was intact (Pennanen et al., 2004, 2006).

The mechanisms contributing to the selective vulnerability of NbM cholinergic neurons in AD are unclear. Using the TUNEL method DNA fragmentation was not observed in the NbM of AD brains, but the apoptotic signal Fas-associated death domain was localized in NbM cholinergic neurons (Wu et al., 2005). Because of their dependence on nerve growth factor, down regulation of TrkA gene expression in NbM cholinergic neurons during the progression of AD is likely to be an important factor (Ginsberg et al., 2006a). A decrease of 3Rtau mRNA relative to 4Rtau mRNA during the progression of AD could ultimately lead to NFT formation (Ginsberg et al., 2006b). However, NFTs may not be directly related to the death of a neuron and tangle-bearing neurons may survive for about 20 years as suggested by a theoretical model based on data from CA1 neurons (Morsch et al., 1999).

In the absence of transgene expression in basal forebrain cholinergic neurons, pathological processes in the cortex and hippocampus could still lead to a functional impairment via retrograde degeneration. Pathological changes in the cortex and hippocampus of pR5 mice include, in addition to neurofibrillary changes, astrocytosis and DNA fragmentation in cortical areas (Götz et al., 2001). Having used ChAT immunostaining the present study did not reveal any difference between basal forebrain cholinergic neurons of pR5 mice and non-tg littermates, however, it does not exclude changes that are beyond detection with the methods used in this study. To the best of our knowledge cholinergic neurons in the basal forebrain have as yet not been investigated by others in tau transgenic mouse models (reviewed in: Cassel et al., 2008). This however has been done in strains overexpressing APP, with and without presenilins, both key proteins involved in AD; these did not find that cortical and hippocampal neuropathology leads to degeneration of ChAT-ir, cholinergic neurons in the basal forebrain (Wong et al., 1999; Hernandez et al., 2001; Boncristiano et al., 2002; German et al., 2003; Perez et al., 2007). In young and middle-aged APP^{swe}/PS1ΔE9 transgenic mice, numbers of cholinergic neurons in the NbM or ChAT optical density measurements were not significantly different when compared to non-tg mice; however, the area of cholinergic neurons in the NbM of old APP^{swe}/PS1ΔE9 transgenic mice was significantly enlarged compared to non-tg mice (Perez et al., 2007). Similar results were reported for the APP23 and PDAPP strains. There was no loss of basal forebrain cholinergic neurons in aged APP23 and PDAPP mice compared to young transgenic mice, suggesting that the loss of cholinergic fibers observed in the cortex and hippocampus of these mice was locally induced by the deposition of beta-amyloid in these areas (Boncristiano et al., 2002; German et al., 2003).

Dystrophic cholinergic terminals in the vicinity of amyloid were observed in AD patients and in mice expressing genetically altered APP with and without presenilin 1 (Wong et al., 1999; Boncristiano et al., 2002; German et al., 2003; Masliah et al., 2003; Köhler et al., 2005). Among different neurotransmitter systems, cholinergic terminals seem to be the most vulnerable (Bell et al., 2006). Despite widespread hyperphosphorylation of tau in the cortex and hippocampus of pR5 mice, we found only a few

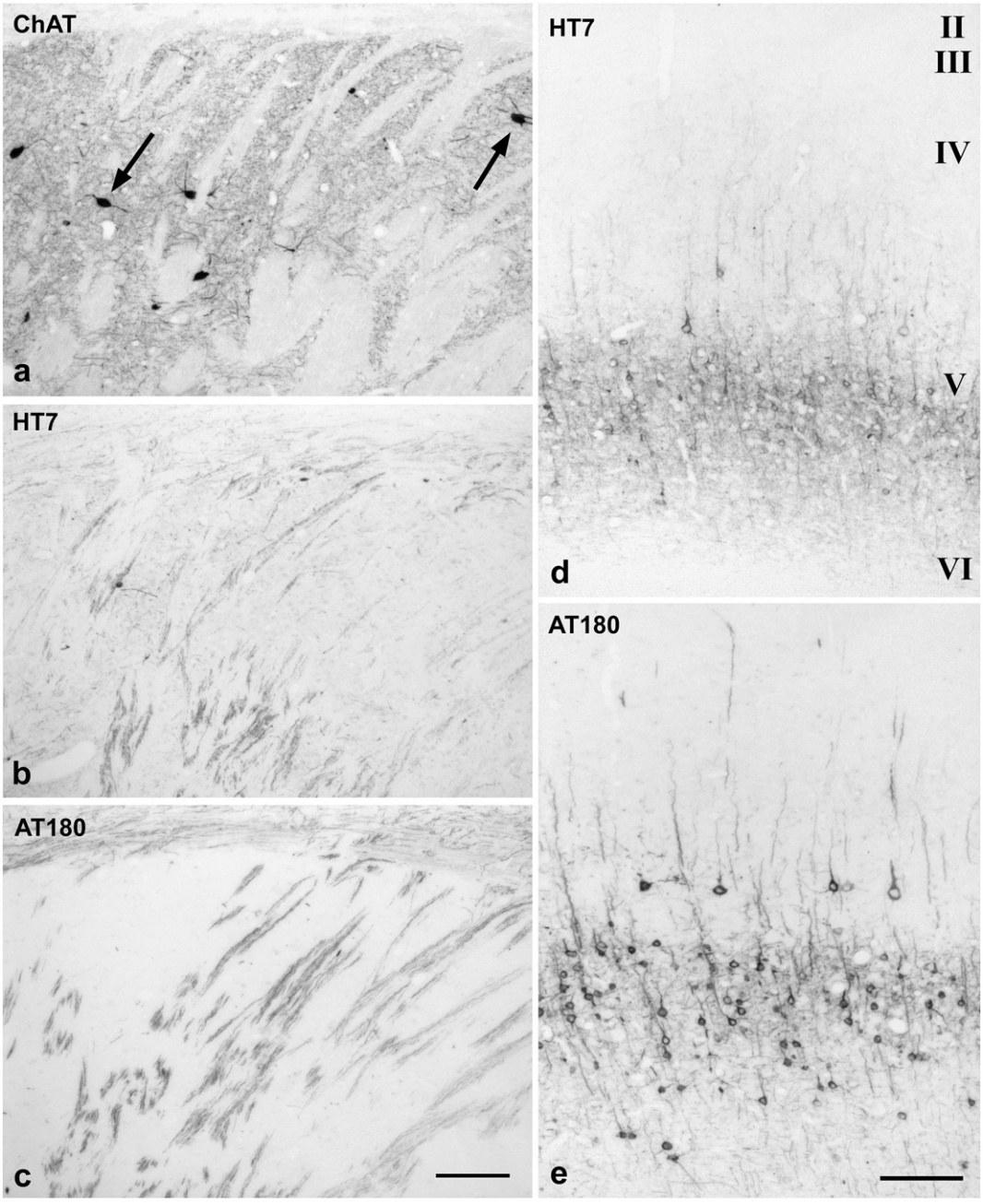

Fig. 10 – Correspondence between htau expression and hyperphosphorylation of tau in the caudate–putamen and cortex of P301L tau transgenic pR5 mice. a, b 4% PFA-fixed, 5 μm thick, coronal sections through the left caudate–putamen and primary somatosensory cortex of a pR5 brain showing (a) ChAT-ir cholinergic interneurons in the caudate–putamen (arrows point to examples) and a fine cholinergic fiber plexus in the matrix which leaves striosomes unstained. (b) HT7-immunoreactivity in the caudate–putamen is confined to fibers. (c) Similar to HT7-immunoreactivity only fibers display the AT180-epitope. (d) Neurons which express htau are located in layer V of the primary somatosensory cortex. Roman numerals indicate cortical layers. (e) The distribution of AT180-ir in the primary somatosensory cortex follows the pattern of transgene expression. Bar a–d 100 μm.

moderately altered cholinergic neurites similar to non-tg littermates. It is unclear whether neurons which contain hyperphosphorylated tau are functionally impaired and whether it would have an effect on their cholinergic innervation. We observed an advanced type of ChAT-ir dystrophic neurite in the basolateral amygdaloid nucleus of pR5 mice that coincides with the presence of many tangle-bearing neurons in this nucleus (Deters et al., 2008). However, there is little neurofibrillary pathology in the lateral amygdaloid nucleus where this type of dystrophic neurite was also observed.

In conclusion, as a consequence of overexpressing P301L mutant htau, pR5 mice develop widespread hyperphosphorylation of tau leading to neurofibrillary lesions mainly in the amygdala and hippocampus. Most of the histological

Table 1 – The table presents a summery of the results from immunohistochemical stainings of the basal forebrain of pR5 mice for choline-acetyl transferase (ChAT) and with antibodies HT7, AT8 and AT180.

Neuronal perikarya in	ChAT	HT7	AT8	AT180
NbM	***	*	*	*
LS, dorsal part	*	*	*	*
LS, intermediate part	***	0	0	0
LS, ventral part	**	0	0	0
MS	***	0	*	*
HDB	***	0	*	**
VDB	***	0	*	**
Caudate–putamen	***	0	0	0

0 none, * a few, ** some, *** many, HDB horizontal limb of the diagonal band of Broca, LS lateral septal nucleus, MS medial septum, NbM nucleus basalis magnocellularis, VDB vertical limb of the diagonal band.

distribution of the aberrant phospho-epitopes investigated in this study closely corresponds to the pattern of selective expression of the transgene produced by the mThy1.2 promoter. Therefore, while pR5 mice faithfully replicate many aspects of the human AD pathology, they do not model the involvement of basal forebrain cholinergic neurons in AD.

4. Experimental procedures

4.1. *Animals*

Transgenic pR5 mice have been previously generated on a B6D2F2 background followed by intercrossing with C57BL/6 mice to establish lines. They express the longest human tau isoform, htau40, together with the pathogenic mutation P301L that has been previously identified in FTD. Transgene expression is driven by a modified version of the mThy1.2 promoter that confers neuronal expression (Götz et al., 2001). For the present study, pR5 mice were further backcrossed to C57/BL6 (obtained from Harlan, Horst, The Netherlands) seven times (in the Department of Anatomy, Cologne, Germany). At 20 months of age, the basal forebrains of eight female heterozygous pR5 mice and six female non-transgenic littermates were analyzed. Animals were kept under standard conditions with food and water ad libitum and were handled according to the guidelines of the animal care committee of the University of Cologne.

4.2. *Antibodies*

The following primary antibodies were used: goat polyclonal antibody to ChAT (Millipore, Schwalbach/Taunus, Germany, catalog # AB144P; diluted 1:200, this antibody was widely used for immunostaining of cholinergic neurons, the data sheet provides a list of 49 references); mouse monoclonal antibody HT7 specific for human tau (amino acids 159–163) (Thermo Scientific Pierce Protein Research Products, Rockford, USA, catalog # MN1000; 1:400); mouse monoclonal antibody AT8 specific for tau phosphorylated at Ser202 and Thr205 (Thermo Scientific Pierce Protein Research Products, Rockford, USA, catalog # MN1020; 1:1000) (Goedert et al., 1995); and mouse monoclonal antibody AT180 specific for tau phosphorylated at Thr231/Ser235 (Thermo Scientific Pierce Protein Research Products, Rockford, USA, catalog # MN1040; 1:1400 and 1:2400) (Goedert et al., 1994).

4.3. *Tissue processing and immunohistochemistry*

Methods of tissue processing and immunohistochemical staining of paraffin sections have recently been published (Köhler, 2010). Sections were pretreated (except for antibody HT7 staining) by boiling for 3×5 min in citrate buffer (pH 6.0) in a microwave oven. The color reaction for ChAT staining was terminated when small processes became visible in the cortex.

4.4. *Double staining*

To demonstrate the expression of htau or hyperphosphorylated tau and cholinergic neurons in the same sections, these were consecutively stained: first with antibodies HT7, AT8 or AT180 and then for ChAT. If combined with HT7 staining, microwave pretreatment for ChAT was omitted and a higher concentration of the ChAT antibody (1:100) was used. Bound AT8/AT180/HT7 antibodies were finally visualized using DAB with nickel enhancement resulting in a deep blue-gray reaction product. Before staining for ChAT, the peroxidase from the previous stain was blocked by incubating the sections in 0.3% H_2O_2 in TBS for 30 min at RT. The ChAT antibody reaction was followed by a peroxidase-coupled anti-goat (1:20, Linaris, Germany) secondary antibody. DAB without nickel enhancement results in a brown reaction product indicating ChAT antibody binding. For double staining of cholinergic terminals and hyperphosphorylated tau ChAT staining was done first followed by staining with antibody AT180.

4.5. *Quantification of ChAT-immunoreactivity in the NbM and septum*

Structures were identified according to the mouse brain atlas of Paxinos and Franklin (2001). ChAT-ir neurons dispersed in the lateral globus pallidus and substantia innominata of both sides were counted in three sections evenly distributed from approximately Bregma positions –0.34 to –1.34 at 400× total magnification if they displayed a visible nucleus. Cholinergic interneurons in the caudate–putamen and cholinergic neurons located on the border between the caudate–putamen and lateral globus pallidus as well as small, weakly stained neurons extending into the lateral hypothalamic area were excluded. ChAT-ir neurons in the medial septum and vertical limb of the diagonal band of Broca were similarly counted in three sections evenly distributed from approximately Bregma positions 1.10 to 0.62. Because there is no distinctive border between the vertical and horizontal limbs of the diagonal band at Bregma positions 1.10 to 0.74, a line drawn perpendicular to the long axis of the medial septum at the level of its outer ventral border was used to delineate the vertical and horizontal limbs of the diagonal band. This led to the inclusion of a few cholinergic neurons in the horizontal limbs of the diagonal band. At Bregma position 0.62 neurons in the medial

septum were clearly separated from neurons in the horizontal limbs of the diagonal band.

To measure the area of ChAT-ir profiles in the lateral globus pallidus/substantia innominata and medial septum, images from the respective areas were taken at 200× total magnification using an Olympus VANOX AHBT3-microscope equipped with an XC-10 digital camera (Olympus Soft Imaging Solutions, Münster, Germany) at Bregma positions –0.7 to –0.94 and 0.86 to 0.74 respectively. Individual ChAT-ir profiles were automatically recognized as "particles" by the cell^F software (Olympus Soft Imaging Solutions, Münster, Germany) according to thresholds set for pixel values of hue, saturation and intensity. The area of the profiles was calculated by the program. Automatic recognition of "particles" by the program was checked and manually corrected if necessary. The lower threshold for saturation was set slightly higher for globus pallidus/substantia innominata measurements, otherwise thresholds were kept constant during all measurements.

4.6. *Digital imaging*

Stained sections were examined with an Olympus VANOX AHBT3-microscope equipped with a XC10 digital camera (Olympus Soft Imaging Solutions, Münster, Germany) or an Olympus BX40-microscope equipped with phase contrast and a ColorView II digital camera (Olympus Soft Imaging Solutions, Münster, Germany). Digital images were processed for color, brightness and contrast using picture publisher 8 (Micrografx) or Adobe Photoshop 5.0. Small tissue damages were retouched without altering the scientific information.

4.7. *Statistical analysis*

The SPSS 16.0 software was used for statistical analysis. Students *T*-test was used for comparison of the means if the data were normally distributed; if not, the Mann–Whitney-*U*-Test was used. *P* values of <0.05 were considered statistically significant.

Acknowledgments

This study was supported by the Hochhaus Foundation of the University of Cologne. The excellent technical assistance of Mrs. M. Dinekov is gratefully acknowledged.

REFERENCES

Baxter, M.G., Holland, P.C., Gallagher, M., 1997. Disruption of decrements in conditioned stimulus processing by selective removal of hippocampal cholinergic input. J. Neurosci. 17, 5230–5236.

Bell, K.F., Ducatenzeiler, A., Ribeiro-da-Silva, A., Duff, K., Bennett, D.A., Cuello, A.C., 2006. The amyloid pathology progresses in a neurotransmitter-specific manner. Neurobiol. Aging 27, 1644–1657.

Bierer, L.M., Haroutunian, V., Gabriel, S., et al., 1995. Neurochemical correlates of dementia severity in Alzheimer's disease: relative importance of the cholinergic deficits. J. Neurochem. 64, 749–760.

Bird, T.D., Nochlin, D., Poorkaj, P., et al., 1999. A clinical pathological comparison of three families with frontotemporal dementia and identical mutations in the tau gene (P301L). Brain 122, 741–756.

Boncristiano, S., Calhoun, M.E., Kelly, P.H., et al., 2002. Cholinergic changes in the APP23 transgenic mouse model of cerebral amyloidosis. J. Neurosci. 22, 3234–3243.

Braak, H., Braak, E., 1991. Neuropathological stageing of Alzheimer-related changes. Acta Neuropathol. 82, 239–259.

Braak, H., Braak, E., 1993. Entorhinal–hippocampal interaction in mnestic disorders. Hippocampus 3 Spec No:239-46.

Bucci, D.J., Conley, M., Gallagher, M., 1999. Thalamic and basal forebrain cholinergic connections of the rat posterior parietal cortex. NeuroReport 10, 941–945.

Caroni, P., 1997. Overexpression of growth-associated proteins in the neurons of adult transgenic mice. J. Neurosci. Meth. 71, 3–9.

Carlsen, J., Záborszky, L., Heimer, L., 1985. Cholinergic projections from the basal forebrain to the basolateral amygdaloid complex: a combined retrograde fluorescent and immunohistochemical study. J. Comp. Neurol. 234, 155–167.

Cassel, J.C., Mathis, C., Majchrzak, M., Moreau, P.H., Dalrymple-Alford, J.C., 2008. Coexisting cholinergic and parahippocampal degeneration: a key to memory loss in dementia and a challenge for transgenic models? Neurodegener. Dis. 5, 304–317.

Chiba, A.A., Bushnell, P.J., Oshiro, W.M., Gallagher, M., 1999. Selective removal of cholinergic neurons in the basal forebrain alters cued target detection. NeuroReport 10, 3119–3123.

Cullen, K.M., Halliday, G.M., 1998. Neurofibrillary degeneration and cell loss in the nucleus basalis in comparison to cortical Alzheimer pathology. Neurobiol. Aging 19, 297–306.

DeKosky, S.T., Harbaugh, R.E., Schmitt, F.A., et al., Intraventricular Bethanecol Study Group, 1992. Cortical biopsy in Alzheimer's disease: diagnostic accuracy and neurochemical, neuropathological, and cognitive correlations. Ann. Neurol. 32, 625–632.

Deters, N., Ittner, L.M., Götz, J., 2008. Divergent phosphorylation pattern of tau in P301L tau transgenic mice. Eur. J. Neurosci. 28, 137–147.

Efange, S.M., Garland, E.M., Staley, J.K., Khare, A.B., Mash, D.C., 1997. Vesicular acetylcholine transporter density and Alzheimer's disease. Neurobiol. Aging 18, 407–413.

Galani, R., Lehmann, O., Bolmont, T., et al., 2002. Selective immunolesions of CH4 cholinergic neurons do not disrupt spatial memory in rats. Physiol. Behav. 76, 75–90.

German, D.C., Yazdani, U., Speciale, S.G., Pasbakhsh, P., Games, D., Liang, C.L., 2003. Cholinergic neuropathology in a mouse model of Alzheimer's disease. J. Comp. Neurol. 462, 371–381.

Ginsberg, S.D., Che, S., Wuu, J., Counts, S.E., Mufson, E.J., 2006a. Down regulation of trk but not p75NTR gene expression in single cholinergic basal forebrain neurons mark the progression of Alzheimer's disease. J. Neurochem. 97, 475–487.

Ginsberg, S.D., Che, S., Counts, S.E., Mufson, E.J., 2006b. Shift in the ratio of three-repeat tau and four-repeat tau mRNAs in individual cholinergic basal forebrain neurons in mild cognitive impairment and Alzheimer's disease. J. Neurochem. 96, 1401–1408.

Goedert, M., Jakes, R., Crowther, R.A., et al., 1994. Epitope mapping of monoclonal antibodies to the paired helical filaments of Alzheimer's disease: identification of phosphorylation sites in tau protein. Biochem. J. 301, 871–877.

Goedert, M., Jakes, R., Vanmechelen, E., 1995. Monoclonal antibody AT8 recognises tau protein phosphorylated at both serine 202 and threonine 205. Neurosci. Lett. 189, 167–169.

Götz, J., Chen, F., Barmettler, R., Nitsch, R.M., 2001. Tau filament formation in transgenic mice expressing P301L tau. J. Biol. Chem. 276, 529–534.

Götz, J., Ittner, L.M., 2008. Animal models of Alzheimer's disease and frontotemporal dementia. Nat. Rev. Neurosci. 9, 532–544.
Götz, J., Götz, N.N., 2009. Animal models for Alzheimer's disease and frontotemporal dementia: a perspective. ASN Neuro 1 (4) pii: e00019.
Gómez-Isla, T., Price, J.L., McKeel Jr, D.W., Morris, J.C., Growdon, J. H., Hyman, B.T., 1996. Profound loss of layer II entorhinal cortex neurons occurs in very mild Alzheimer's disease. J. Neurosci. 16, 4491–4500.
Gonzalez de Aguilar, J.L., Loeffler, J.P., Boutillier, A.L., 2008. Lesions and genes: on the edge of improved isomorphic models for Alzheimer's disease? Neurodegener. Dis. 5, 318–320.
Gritti, I., Manns, I.D., Mainville, L., Jones, B.E., 2003. Parvalbumin, calbindin, or calretinin in cortically projecting and GABAergic, cholinergic, or glutamatergic basal forebrain neurons of the rat. J. Comp. Neurol. 458, 11–31.
Grueninger, F., Bohrmann, B., Czech, C., et al., 2010. Phosphorylation of Tau at S422 is enhanced by Abeta in TauPS2APP triple transgenic mice. Neurobiol. Dis. 37, 294–306.
Härtig, W., Stieler, J., Boerema, A.S., et al., 2007. Hibernation model of tau phosphorylation in hamsters: selective vulnerability of cholinergic basal forebrain neurons—implications for Alzheimer's disease. Eur. J. Neurosci. 25, 69–80.
Hernandez, D., Sugaya, K., Qu, T., McGowan, E., Duff, K., McKinney, M., 2001. Survival and plasticity of basal forebrain cholinergic systems in mice transgenic for presenilin-1 and amyloid precursor protein mutant genes. NeuroReport 12, 1377–1384.
Houdebine, L.M., 2002. The methods to generate transgenic animals and to control transgene expression. J. Biotechnol. 98, 145–160.
Hutton, M., Lendon, C.L., Rizzu, P., et al., 1998. Association of missense and 5′-splice-site mutations in tau with the inherited dementia FTDP-17. Nature 393, 702–705.
Hyman, B.T., Van Hoesen, G.W., Damasio, A.R., Barnes, C.L., 1984. Alzheimer's disease: cell-specific pathology isolates the hippocampal formation. Science 225, 1168–1170.
Hyman, B.T., Van Hoesen, G.W., Damasio, A.R., 1990. Memory-related neural systems in Alzheimer's disease: an anatomic study. Neurology 40, 1721–1730.
Iraizoz, I., Guijarro, J.L., Gonzalo, L.M., de Lacalle, S., 1999. Neuropathological changes in the nucleus basalis correlate with clinical measures of dementia. Acta Neuropathol. 98, 186–196.
Ittner, L.M., Fath, T., Ke, Y.D., et al., 2008. Parkinsonism and impaired axonal transport in a mouse model of frontotemporal dementia. Proc. Natl. Acad. Sci. U. S. A. 105, 15997–16002.
Ittner, L.M., Ke, Y.D., Götz, J., 2009. Phosphorylated Tau interacts with c-Jun N-terminal kinase-interacting protein 1 (JIP1) in Alzheimer disease. J. Biol. Chem. 284, 20909–20916.
Kitt, C.A., Höhmann, C., Coyle, J.T., Price, D.L., 1994. Cholinergic innervation of mouse forebrain structures. J. Comp. Neurol. 341, 117–129.
Köhler, C., Ebert, U., Baumann, K., Schröder, H., 2005. Alzheimer's disease-like neuropathology of gene-targeted APP-SLxPS1mut mice expressing the amyloid precursor protein at endogenous levels. Neurobiol. Dis. 20, 528–540.
Köhler, C.N., 2010. The actin-binding protein caldesmon is in spleen and lymph nodes predominately expressed by smooth muscle cells, reticular cells, and follicular dendritic cells. J. Histochem. Cytochem. 58, 183–193.
Kurt, M.A., Davies, D.C., Kidd, M., et al., 2001. Neurodegenerative changes associated with beta-amyloid deposition in the brains of mice carrying mutant amyloid precursor protein and mutant presenilin-1 transgenes. Exp. Neurol. 171, 59–71.
Lewis, J., McGowan, E., Rockwood, J., et al., 2000. Neurofibrillary tangles, amyotrophy and progressive motor disturbance in mice expressing mutant (P301L) tau protein. Nat. Genet. 25, 402–405.
Masliah, E., Alford, M., Adame, A., et al., 2003. Abeta1-42 promotes cholinergic sprouting in patients with AD and Lewy body variant of AD. Neurology 61, 206–211.
McGehee, D.S., Heath, M.J., Gelber, S., Devay, P., Role, L.W., 1995. Nicotine enhancement of fast excitatory synaptic transmission in CNS by presynaptic receptors. Science 269, 1692–1696.
McGeorge, A.J., Faull, R.L., 1989. The organization of the projection from the cerebral cortex to the striatum in the rat Neuroscience 29, 503–537.
McKinney, M., Coyle, J.T., Hedreen, J.C., 1983. Topographic analysis of the innervation of the rat neocortex and hippocampus by the basal forebrain cholinergic system. J. Comp. Neurol. 217, 103–121.
Mesulam, M., Shaw, P., Mash, D., Weintraub, S., 2004. Cholinergic nucleus basalis tauopathy emerges early in the aging-MCI-AD continuum. Ann. Neurol. 55, 815–828.
Mirra, S.S., Murrell, J.R., Gearing, M., et al., 1999. Tau pathology in a family with dementia and a P301L mutation in tau. J. Neuropathol. Exp. Neurol. 58, 335–345.
Miyasaka, T., Morishima-Kawashima, M., Ravid, R., 2001. Selective deposition of mutant tau in the FTDP-17 brain affected by the P301L mutation. J. Neuropathol. Exp. Neurol. 60, 872–884.
Morsch, R., Simon, W., Coleman, P.D., 1999. Neurons may live for decades with neurofibrillary tangles. J. Neuropathol. Exp. Neurol. 58, 188–197.
Murakami, T., Paitel, E., Kawarabayashi, T., et al., 2006. Cortical neuronal and glial pathology in TgTauP301L transgenic mice: neuronal degeneration, memory disturbance, and phenotypic variation. Am. J. Pathol. 169, 1365–1375.
Nagai, T., Kimura, H., Maeda, T., McGeer, P.L., Peng, F., McGeer, E.G., 1982. Cholinergic projections from the basal forebrain of rat to the amygdala. J. Neurosci. 2, 513–520.
Naito, A., Kita, H., 1994. The cortico-pallidal projection in the rat: an anterograde tracing study with biotinylated dextran amine. Brain Res. 653, 251–257.
Nasreddine, Z.S., Loginov, M., Clark, L.N., et al., 1999. From genotype to phenotype: a clinical pathological, and biochemical investigation of frontotemporal dementia and parkinsonism (FTDP-17) caused by the P301L tau mutation. Ann. Neurol. 45, 704–715.
Paxinos, G., Franklin, K.B.J., 2001. The Mouse Brain in Stereotaxic Coordinates. Academic press, Second edition.
Pearson, R.C., Sofroniew, M.V., Cuello, A.C., et al., 1983. Persistence of cholinergic neurons in the basal nucleus in a brain with senile dementia of the Alzheimer's type demonstrated by immunohistochemical staining for choline acetyltransferase. Brain Res. 289, 375–379.
Pennanen, L., Welzl, H., D'Adamo, P., Nitsch, R.M., Götz, J., 2004. Accelerated extinction of conditioned taste aversion in P301L tau transgenic mice. Neurobiol. Dis. 15, 500–509.
Pennanen, L., Wolfer, D.P., Nitsch, R.M., Götz, J., 2006. Impaired spatial reference memory and increased exploratory behavior in P301L tau transgenic mice. Genes Brain Behav. 5, 369–379.
Perez, S.E., Dar, S., Ikonomovic, M.D., DeKosky, S.T., Mufson, E.J., 2007. Cholinergic forebrain degeneration in the APPswe/PS1DeltaE9 transgenic mouse. Neurobiol. Dis. 28, 3–15.
Perry, E.K., Blessed, G., Tomlinson, B.E., et al., 1981. Neurochemical activities in human temporal lobe related to aging and Alzheimer-type changes. Neurobiol. Aging 2, 251–256.
Ramsden, M., Kotilinek, L., Forster, C., et al., 2005. Age-dependent neurofibrillary tangle formation, neuron loss, and memory impairment in a mouse model of human tauopathy (P301L). J. Neurosci. 25, 10637–10647.
Reed, L.A., Wszolek, Z.K., Hutton, M., 2001. Phenotypic correlations in FTDP-17. Neurobiol. Aging 22, 89–107.
Rhein, V., Song, X., Wiesner, A., et al., 2009. Amyloid-beta and tau synergistically impair the oxidative phosphorylation system in

triple transgenic Alzheimer's disease mice. Proc. Natl. Acad. Sci. U. S. A. 106, 20057–20062.
Saper, C.B., German, D.C., White III, C.L., 1985. Neuronal pathology in the nucleus basalis and associated cell groups in senile dementia of the Alzheimer's type: possible role in cell loss. Neurology 35, 1089–1095.
Sarter, M., Bruno, J.P., Givens, B., 2003. Attentional functions of cortical cholinergic inputs: what does it mean for learning and memory? Neurobiol. Learn. Mem. 80, 245–256.
Sassin, I., Schultz, C., Thal, D.R., et al., 2000. Evolution of Alzheimer's disease-related cytoskeletal changes in the basal nucleus of Meynert. Acta Neuropathol. 100, 259–269.
Satoh, K., Armstrong, D.M., Fibiger, H.C., 1983. A comparison of the distribution of central cholinergic neurons as demonstrated by acetylcholinesterase pharmacohistochemistry and choline acetyltransferase immunohistochemistry. Brain Res. Bull. 11, 693–720.
Su, B., Wang, X., Drew, K.L., Perry, G., Smith, M.A., Zhu, X., 2008. Physiological regulation of tau phosphorylation during hibernation. J. Neurochem. 105, 2098–2108.
Swanson, L.W., Cowan, W.M., 1979. The connections of the septal region in the rat. J. Comp. Neurol. 186, 621–655.
Wallace, H., Ansell, R., Clark, J., McWhir, J., 2000. Pre-selection of integration sites imparts repeatable transgene expression. Nucleic Acids Res. 28, 1455–1464.
Whitehouse, P.J., Price, D.L., Struble, R.G., Clark, A.W., Coyle, J.T., Delon, M.R., 1982. Alzheimer's disease and senile dementia: loss of neurons in the basal forebrain. Science 215, 1237–1239.
Whitwell, J.L., Jack Jr, C.R., Boeve, B.F., et al., 2009. Atrophy patterns in IVS10+16, IVS10+3, N279K, S305N, P301L, and V337M MAPT mutations. Neurology 73, 1058–1065.
Witter, M.P., 1993. Organization of the entorhinal–hippocampal system: a review of current anatomical data. Hippocampus 3 Spec No:33-44.
Wong, T.P., Debeir, T., Duff, K., Cuello, A.C., 1999. Reorganization of cholinergic terminals in the cerebral cortex and hippocampus in transgenic mice carrying mutated presenilin-1 and amyloid precursor protein transgenes. J. Neurosci. 19, 2706–2716.
Wszołek, Z.K., Słowiński, J., Golan, M., Dickson, D.W., 2005. Frontotemporal dementia and parkinsonism linked to chromosome 17. Folia Neuropathol. 43, 258–270.
Wu, C.K., Thal, L., Pizzo, D., Hansen, L., Masliah, E., Geula, C., 2005. Apoptotic signals within the basal forebrain cholinergic neurons in Alzheimer's disease. Exp. Neurol. 195, 484–496.
Zaborszky, L., Gaykema, R.P., Swanson, D.J., Cullinan, W.E., 1997. Cortical input to the basal forebrain. Neuroscience 79, 1051–1078.